The effects of the mechanical performance and alignment of the Atacama Cosmology Telescope on the sensitivity of microwave observations

A. D. Hincks,[a] P. A. R. Ade,[b] C. Allen,[c] M. Amiri,[d] J. W. Appel,[a] E. S. Battistelli,[d, e] B. Burger,[d] J. A. Chervenak,[c] A. J. Dahlen,[a] S. Denny,[a] M. J. Devlin,[f] S. R. Dicker,[f] W. B. Doriese,[g] R. Dünner,[h] T. Essinger-Hileman,[a] R. P. Fisher,[a] J. W. Fowler,[a] M. Halpern,[d] P. C. Hargrave,[b] M. Hasselfield,[d] G. C. Hilton,[g] K. D. Irwin,[g] N. Jarosik,[a] M. Kaul,[f] J. Klein,[f] J. M. Lau,[i] M. Limon,[j] R. H. Lupton,[k] T. A. Marriage,[k] K. L. Martocci,[l] P. Mauskopf,[b] S. H. Moseley,[c] C. B. Netterfield,[m] M. D. Niemack,[a] M. R. Nolta,[n] L. Page,[a] L. P. Parker,[a] A. J. Sederberg,[a] S. T. Staggs,[a] O. R. Stryzak,[a] D. S. Swetz,[f] E. R. Switzer,[a] R. J. Thornton,[f] C. Tucker,[b] E. J. Wollack,[c] and Y. Zhao[a]

[a]Dept. of Physics, Jadwin Hall, Princeton University, Princeton, NJ 08544-0708, USA;
[b]Dept. of Physics & Astronomy, Cardiff University, 5 The Parade, Cardiff, CF24 3AA, UK;
[c]Code 665, NASA Goddard Space Flight Center, Greenbelt, MD 20771, USA;
[d]Dept. of Physics and Astronomy, University of British Columbia, Vancouver, BC V6T 1Z1, Canada;
[e]Dept. of Physics, University of Rome "La Sapienza", Piazzale Aldo Moro 5, I-00185 Rome, Italy;
[f]Dept. of Physics and Astronomy, University of Pennsylvania, 209 South 33rd Street, Philadelphia, PA 19104, USA;
[g]National Institute of Standards and Technology, 325 Broadway, Boulder, CO 80305, USA;
[h]Dept. de Astronomía y Astrofísica, Facultad de Física, Pontificia Universidad Católica de Chile, Casilla 306, Santiago 22, Chile;
[i]Stanford University Physics Dept., 382 Via Pueblo Mall, Stanford, CA 94305, USA;
[j]Columbia Astrophysics Laboratory, 550 W. 120th St. Mail Code 5247, New York, NY 10027, USA;
[k]Dept. of Astrophysical Sciences, Peyton Hall, Princeton University, Princeton, NJ 08544, USA;
[l]Dept. of Physics, City University of New York, 365 5th Avenue, Suite 6412, New York, NY 10016, USA;
[m]Dept. of Physics, University of Toronto, 60 St. George Street, Toronto, ON M5S 1A7, Canada;
[n]Canadian Institute for Theoretical Astrophysics, 60 St. George St, University of Toronto, Toronto, ON M5S 3H8, Canada

ABSTRACT

The Atacama Cosmology Telescope is a six meter, off-axis Gregorian telescope for measuring the cosmic microwave background at arcminute resolutions. The Millimeter Bolometer Array Camera (MBAC) is its current science instrument. Erected in the Atacama Desert of Chile in early 2007, it saw first light with the MBAC on 22 October 2007. In this paper we review its performance after one month of observing, focusing in particular on issues surrounding the alignment of the optical system that impact the sensitivity of the experiment. We discuss

Send correspondence to ahincks@Princeton.EDU.

Millimeter and Submillimeter Detectors and Instrumentation for Astronomy IV
edited by William D. Duncan, Wayne S. Holland, Stafford Withington, Jonas Zmuidzinas
Proc. of SPIE Vol. 7020, 70201P, (2008) · 0277-786X/08/$18 · doi: 10.1117/12.790020

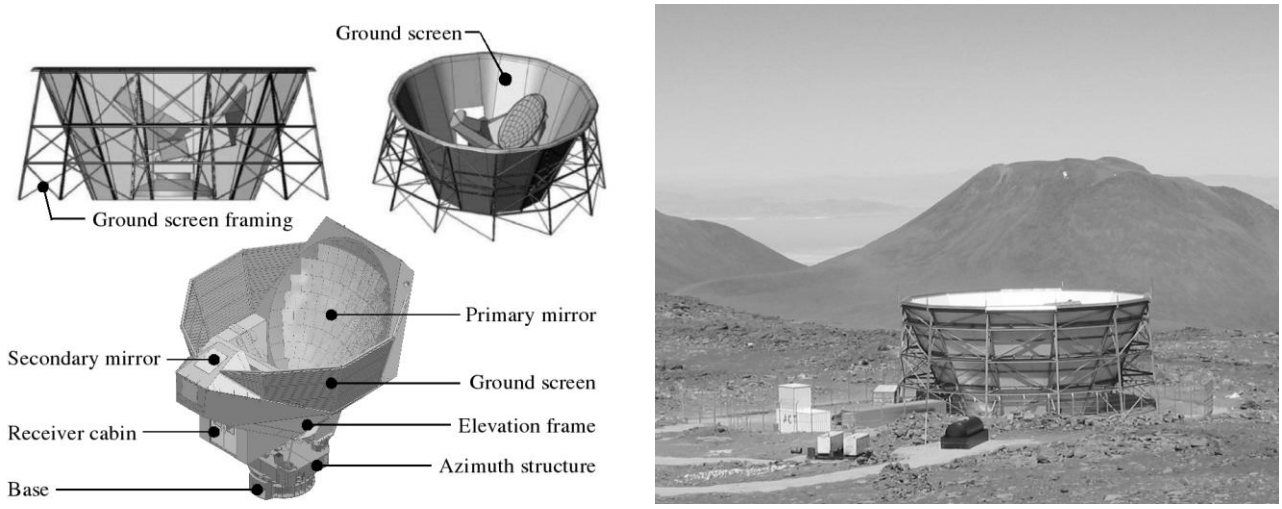

Figure 1. The Atacama Cosmology Telescope. *Left:* Drawings of the telescope. The full height of the telescope is 12 m The entire upper structure ("azimuth structure" and above) rotates during scanning motion. The focus of the secondary mirror is below the primary mirror in the receiver cabin. The telescope is surrounded by a ground screen to block radiation from the earth. Another ground screen is mounted on the sides of the telescope itself. *Right:* The telescope in the Atacama Desert in Chile. The generators, fuel tank and shipping containers for storage, equipment and office space also appear in this photograph.

the telescope motion, pointing, and susceptibility to thermal distortions. We describe the mirror alignment procedure, which has yielded surface deviations of 31 μm rms on the primary and 10 μm rms on the secondary. Observations of planets show that the optical performance is consistent with the telescope design parameters. Preliminary analysis measures a solid angle of about 215 nanosteradians with a full width at half maximum of 1.44 arcminutes at 145 GHz.

Keywords: Microwave Telescopes, CMB Observations

1. INTRODUCTION

The Atacama Cosmology Telescope (ACT) is a six meter, off-axis Gregorian telescope designed for observing the cosmic microwave background (CMB) at arcminute resolutions.[1,2] It was built by AMEC Dynamic Structures Ltd.* (DS) in Port Coquitlam, British Columbia, and installed on Cerro Toco in the Atacama Desert of northern Chile in 2007 with on-site assistance from Con Pax.† The low levels of water vapor and the high altitude (5190 m) make this location ideal for millimeter astronomy.[3] Fig. 1 shows drawings and a photograph of the telescope. Table 1 summarizes its important parameters.

Following the installation a period of commissioning began. Two items in particular were important to assess the performance of the telescope: the tuning of the telescope motion and the alignment of the primary and secondary mirror panels. Extensive work on both of these areas ensured that the design specifications were met by the austral spring, in time for the arrival of the receiver in October.

The receiver is called the Millimeter Bolometer Array Camera (MBAC).[4–6] For the 2007 season, it contained a 1024-element array of transition edge sensors (TES) operating at 145 GHz. Two more arrays at 220 GHz and 280 GHz will be installed in June of 2008 for subsequent observations.[7–10] It saw first light on 22 October 2007 and continued observing until mid-December. Analysis of these data is ongoing.

*Formerly owned by AMEC Inc., it was acquired by Empire Industries Ltd. in 2007 and is now named Empire Dynamic Structures Ltd. Business address: 1515 Kingsway Ave., Port Coquitlam BC V3C 1S2, Canada. Internet URL: http://www.dynamicstructuresltd.com.

†Internet URL: http://www.con-pax.cl.

Telescope Properties		**Location**	
Total maximum height	12 m	Altitude	5190 m
Ground screen height	13 m	Longitude	67°47′15″W
Total mass	52 t	Latitude	22°57′31″S
Mass of moving structure	40 t		
Optics		**Motion**	
Focal ratio	~ 2.5	Azimuth range	$-220° - +220°$
Field of view at focus[a]	$\sim 1°^2$	Maximum azimuth speed	$2°/s$
Primary mirror maximum diameter	6 m	Maximum azimuth acceleration	$10°/s^2$
Number of primary mirror panels	71	Elevation range	$30.5° - 60°$
Secondary mirror maximum diameter	2 m	Maximum elevation speed	$0.2°/s$
Number of secondary mirror panels	11		

[a]Defined as the region with 280 GHz Strehl ratio > 0.9, according to design.

Table 1. Important telescope parameters. The optics are discussed in more detail in Ref. 6.

This paper is one in a series of papers in these proceedings which describe the technical ascpects of the ACT: the MBAC receiver, the detectors, and the data acquisition systems.[4, 5, 7, 10, 11] In this paper we discuss the telescope's mechanical performance after its first season. Section 2 reports on the quality of the telescope motion; Section 3 describes our panel alignment procedure and surface rms; Section 4 shows the diurnal thermal changes that the telescope structure undergoes; Section 5 outlines the telescope pointing model. In Section 6 we present a preliminary beam map. We conclude in Section 7.

2. TELESCOPE MOTION

Most CMB instruments observe in a manner such that the input celestial signal is at a frequency high enough to separate it from $1/f$ noise in the data analysis. The ACT does this by rotating the telescope back and forth in azimuth. The specifications called for constant-velocity motion with rapid turn-arounds at the endpoints of the scans. The scan was to be smooth enough that the pointing rms was at most 6 arcseconds from the commanded position. Given that the moving part of the telescope, which includes all of the optics, weighs about 40 metric tons, this was a considerable engineering challenge.

The motion system was subcontracted to KUKA, a robotics systems company.[‡] The hardware—resolvers, encoders, current drivers, etc.—as well as the motion control software are commercial products. Significant extensions to the KUKA software were required to meet the stringent demands of our instrument. The control software is a proprietary package, and as such, the ACT collaboration has little control over the details of its operation. Motion is commanded to the KUKA system over a combination of ethernet and DeviceNet, a robotics communication standard.[11, 12]

A pair of 27-bit Heidenhain absolute encoders on the azimuth and elevation axes are used to monitor the telescope position. The KUKA control system uses an identical pair of encoders mounted next to these, but their readout and control loop is kept strictly separate. Clinometers measure the tilt of the base and the rotating structure. Accelerometers are mounted near the secondary mirror and at four positions up the center of the primary mirror. The readout of all these instruments is synchronized to detector data to within 5 μs.[11]

A maximum scan speed of $2°/s$ with turn-arounds of 400 ms (or $10°/s^2$) has been achieved. Fig. 2 shows velocity and position residual plots for motion at the maximum speed and acceleration. The pointing error during the constant-velocity portion of the scan is well within the 6 arcsecond pointing requirement. A bobbing

[‡]Internet URL: http://www.kuka.com.

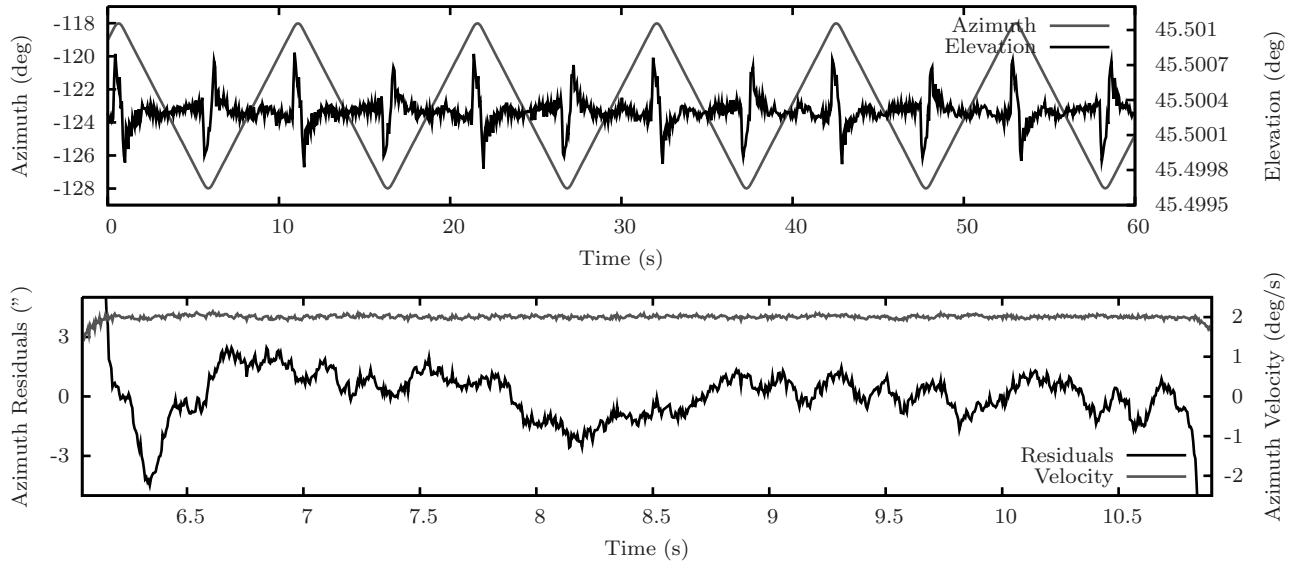

Figure 2. Motion quality for 2°/s azimuthal scans, the maximum scan speed. *Top:* Azimuth and elevation encoder readings. At the end of each scan, the elevation axis bobs by about 0.001° or 3.5 arcseconds, well within the 6 arcsecond pointing requirement. *Bottom:* Residuals of the azimuth position and the azimuth velocity for a single scan in one direction. The residuals are from fitting a straight line to the azimuth data. The velocity is calculated by taking the time-derivative of the azimuth. The small-amplitude ~ 5 Hz frequency in the residuals is driven by the control loop.

in elevation of about 3.5 arcseconds occurs at the end of the turn-around. Additionally, there is an overshoot in azimuth at the beginning of the scans (at about 6.3 s in Fig. 2 (*bottom*)). Though this coupling sometimes encroaches beyond the 6 arcsecond tolerance, the control loop damps it out within 200 ms so that it is not a significant concern. To achieve the best motion profile, such as shown in Fig. 2, it is necessary to warm up the motors and gears by running azimuthal scans for about forty-five minutes.

Due to considerations of the optical time constants of the MBAC detectors, data taken during the 2007 observations used 1°/s scans. At this speed the smoothness of the scans is improved: the post-acceleration azimuth overshoot all but disappears and the residuals are less than 2 arcseconds.

3. MIRROR SURFACE ALIGNMENT

Both of the telescope's mirrors consist of segmented aluminum panels manufactured by Forcier Machine Design:[§] 71 for the primary and 11 for the secondary. The primary panels are roughly rectangular, measuring about 65×85 cm, and are laid out in eight rows (as depicted in Fig. 4). The secondary reflector consists of ten trapezoidal panels measuring about 35×75 cm at the widest points, arranged in a petal configuration around a central panel, about 50×80 cm. Individual panels weight about 10 kg.

Each panel is attached to the mirror back-up structure (BUS) by four connectors, one at each corner, about 6 cm from the panel edge. The connectors have two bolts, accessible from the back side of the BUS, which can be manually turned to make coarse and fine adjustments to the panel position in the direction normal to the mirror surface. Coarse adjustments move the connector 529 μm per turn, while fine adjustments yield 117 μm per turn. Fig. 3 shows drawings of a primary mirror panel and a connector.

The surface rms of each panel is 3 μm, much smaller than the actual rms of the overall surface, which is dominated by the relative alignment of the panels. The surface tolerance affects the forward gain G of the instrument, which is defined as

[§]Business address: 123 Marshall Ave, Petaluma, CA 94952, USA.

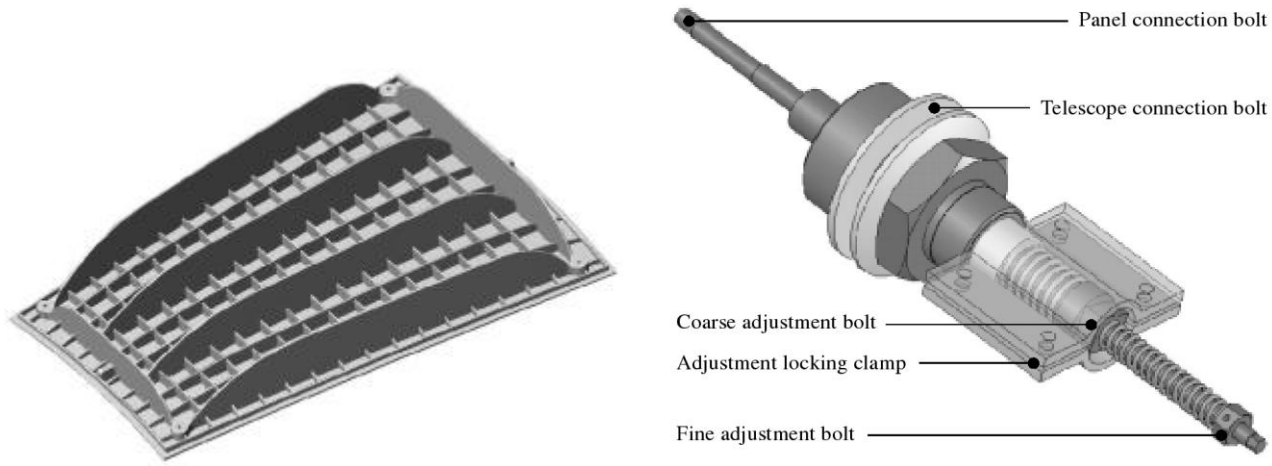

Figure 3. Drawings of a mirror panel and connector. *Left:* A primary mirror panel, viewed from the back. The size is about 65×85 cm. The panel is connected to the telescope at the four corners. *Right:* A panel connector. The large, central telescope connection bolt is secured to the mirror back-up structure (BUS) and the panel connection bolt attaches to the corner of the panel. Coarse and fine adjustment bolts located on the back side of the BUS move the panel connection bolt in and out a distance of 529 μm and 117 μm, respectively. An adjustment locking clamp secures the adjusters in place to prevent them from slipping. The total length of the connector is about 45 cm.

$$G = \frac{4\pi}{\Omega_A} \quad ; \quad \Omega_A = \iint_{4\pi} P_n(\theta, \phi) d\Omega, \tag{1}$$

where Ω_A, the integral over the normalized antenna power P_n, is the beam solid angle.[13] The forward gain for an ideal antenna, G_0, is degraded by the presence of surface inaccuracies. The Ruze condition[14] relates the surface rms to this loss of forward gain:

$$G = G_0 \exp\left[-\left(4\pi\sigma/\lambda\right)^2\right], \tag{2}$$

where σ is the surface tolerance and λ is the observed wavelength. In optical astronomy, G/G_0 is known as the Strehl ratio when $4\pi\sigma/\lambda$ represents the wavefront phase error.[15] Eq. 2 assumes that the scales contributing to the rms are small compared to the antenna diameter; more precisely, higher order terms in Eq. 2 go as the square of the ratio of the rms scale to the antenna diameter. Since our panel size (~ 0.5 m) is about 10% of the primary mirror diameter (~ 6 m), it is appropriate to use this expression to guide our assessment of the panel alignment. Specifically, for our highest frequency (280 GHz), we require an rms of 30 μm for $G/G_0 \approx 90\%$.

We employed a laser tracker manufactured by Faro[¶] to measure the relative alignment of our reflector panels. This instrument uses a laser to determine the distance to a retroreflector. Servo motors allow it to automatically track the retroreflector. The tracker can be mounted on the telescope structure between the primary and secondary mirrors, where it has a full view of both surfaces. The reflector surfaces are then measured by manually holding a retroreflector against the four corners of each panel.

In addition to measuring the primary and secondary panel alignments, the laser tracker is used to determine the relative positions of the optics. The secondary mirror position relative to the primary mirror is measured and adjusted as necessary. Similarly, it is used to measure the position of the MBAC relative to the primary and secondary mirrors.

[¶]Internet URL: http://www.faro.com.

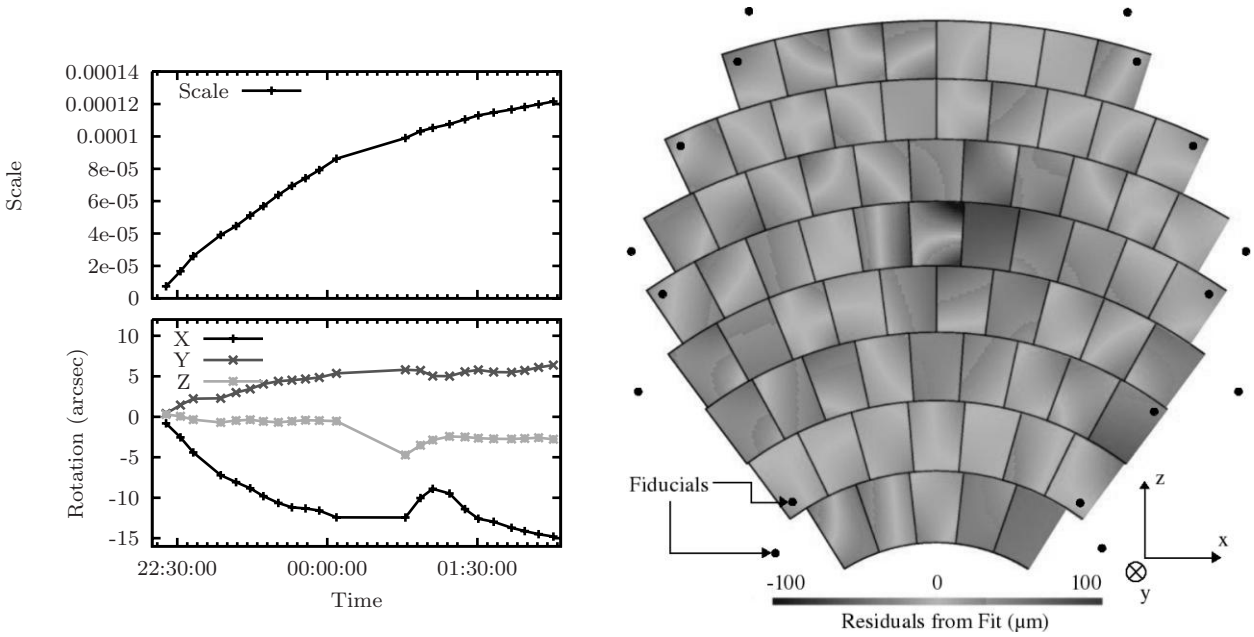

Figure 4. Analysis of the primary mirror surface quality. *Left:* Thermal changes of the mirror during the panel survey, as measured by the fiducial points, and referenced to the first fiducial measurements of the survey. The top plot shows the overall scale of the mirror, i.e., the mirror size scales as $(1 - a)$, where a is the plotted scale. The bottom plot shows how the mirror rotates about a right-handed coordinate system with $\hat{\mathbf{z}}$ pointing vertically upward, $\hat{\mathbf{y}}$ pointing toward the primary mirror, and $\hat{\mathbf{x}}$ pointed horizontally *Right:* The residuals of the aligned primary mirror (on 19 Oct. 2007) from the required ellipsoid surface. Darker regions are furthest out of alignment and lighter regions are well aligned. The solid circles show the approximate positions of the fiducial retroreflectors (see text). The total rms is 31 μm.

Completing a survey of all the panels on both mirrors takes about four hours. Ambient temperature variations on that time scale can cause large-scale thermal expansions and contractions of the telescope structure on the order of hundreds of microns across the primary surface. To account for this deformation, we fix retroreflectors at fiducial positions around the boundaries of the primary and secondary mirrors, some on the panels themselves and some on the frame beyond the edge of the reflector surfaces. Their approximate positions are shown in Fig. 4 (*right*). Between sets of panel measurements, which were done six panels at a time, the positions of these fiducial points are measured. This allows us to model the thermal stretching of the surface and remove this drift from the measured panel positions. The model includes a translation, rotation and global scaling of the surface. Fig. 4 (*left*) shows a selection of these variables during a survey.

Given a set of fiducial-corrected panel measurements, we perform a least-squares best fit to the functional form of our mirror design (see Ref. 6 for the formulae). The residuals from this fit prescribe adjustments to be made to the connectors of each panel.

The surface errors are reduced by an iterative series of panel measurements and adjustments. After three such iterations we achieved an rms of 31 μm and 10 μm on the primary and secondary surfaces, respectively. These values are dominated by the systematic error of the laser tracker's measurements and the uncertainty of fiducial correction; for the primary mirror, this combined error was 27 μm. Fig. 4 (*right*) shows the quality of the primary mirror surface after this alignment.

In preparation for the 2008 observing season, another series of panel measurements and adjustments were performed. Before any adjustments were made, both the primary and the secondary surfaces were measured to have an rms of 35 μm. This indicates that the primary surface retained its tolerance well over the seven months since the previous adjustments. The cause of the change in the secondary mirror is under investigation. Subsequent adjustments aligned the primary surface to at least 31 μm and the secondary surface to 12 μm.

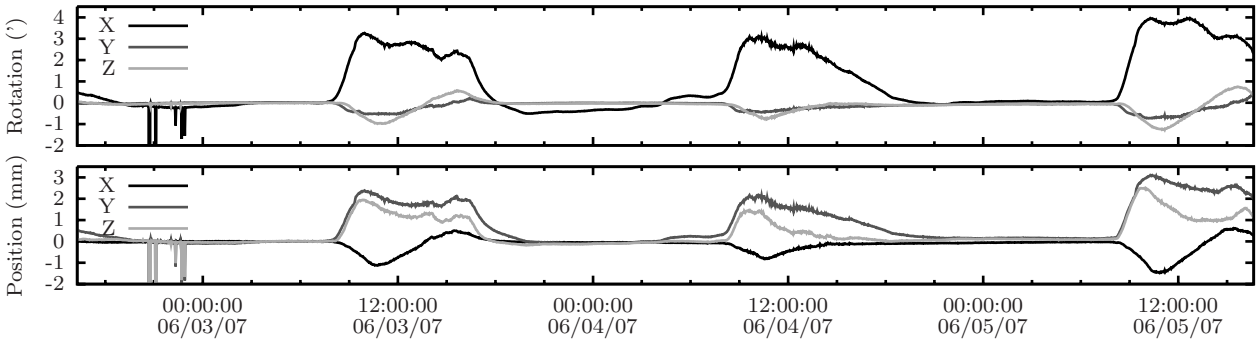

Figure 5. The difference in the motion between the primary and secondary mirrors as measured by the fiducial points over three days. The (x, y, z) coordinate system is described in Fig. 4. On these dates, sunrise was at about 7:05 and sunset at 17:50. The structure is most unstable between these times. *Top:* The differences in rotation about the three axes. *Bottom:* The differences in position.

4. DIURNAL THERMAL EFFECTS

The telescope optics are poorest near sunset and sunrise, when the rapidly changing ambient temperature causes the largest thermal deformations.

To quantify the relative diurnal positions of the primary and secondary mirrors, we used the Faro laser tracker to take continuous measurements over several days of the primary and secondary fiducial points. The six parameter model described in Sec. 3 was applied to both the primary and secondary fiducial points.

Fig. 5 shows the relative rotations and translations of the primary and secondary mirrors. The structure is most stable during the night hours. The most rapid changes take place about an hour after sunrise and an hour before sunset, settling down about two hours after sunset.

Analysis of the point-spread function of planet measurements taken during the night and in the morning gives further insight into the thermal effects on the optical quality. After sunrise, the solid angle and asymmetry of the beam increases substantially. Thus, not only are the primary and secondary moving relative to each other, but the surface rms of the mirrors degrades considerably after sunrise. However, it is important to note that the telescope recovers the correct position each night and that the mirror surfaces regain their alignment.

Our useable data from the 2007 observations were therefore limited to the night hours. For the coming 2008 season, we will take two steps in an attempt to lengthen the period of structural stability. First, we will re-coat the surface of the telescope (excepting the mirrors) with a paint which is more emissive in the infrared to minimize heating. Second, we will install a lightweight sun-shield over the back of the primary mirror BUS. The shield will be a large polypropylene mesh suspended about 25 cm from the surface of the BUS by an aluminum scaffold, itself attached to the BUS. The rising sun will strike the shield instead of the BUS, which is expected to lessen and delay the heating of the telescope structure to allow for observations longer into the daylight hours.

5. TELESCOPE POINTING

Venus, Mars, Saturn, and Uranus were observed about two hundred times altogether during the 2007 season. By comparing the telescope position reported by the azimuth and elevation encoders with the planets' true positions as determined from ephemerides, we can develop a pointing model which depends on physical parameters of the telescope. The parameters with significant contributions to the model are: the offset in the azimuth encoder, the tilt of the azimuth plane from the horizontal, and the cant of the elevation axis out of the azimuth plane. Additionally, as shown in Section 4, thermal contraction and expansion changes the relative angle between the primary and secondary mirrors. This has the effect of introducing a temperature dependence in the elevation pointing.

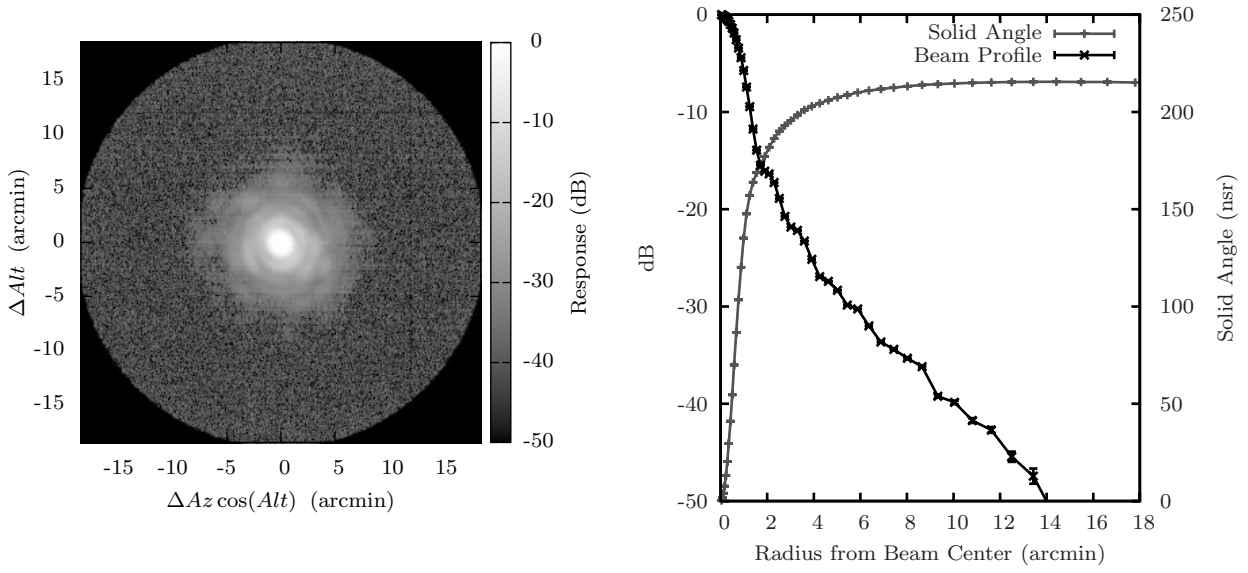

Figure 6. A map and beam profile of Saturn taken on 16 Nov. 2008 at 145 GHz. *Left:* The map, created by coadding all working detectors for one six-minute observation, after removing the $1/f$ drift. The response is plotted as dB referenced to the peak of the planet. *Right:* The beam profile and accumulated solid angle for this map. Error bars represent statistical uncertainties and do not account for systematic errors. The beam profile is averaged in concentric rings from the center and hence blurs any asymmetry in the beam. Beyond about 10 arcminutes, systematic errors in the background subtraction make the profile inaccurate. The FWHM is about 1.44 arcminutes and the solid angle is about 215 nanosteradians (nsr).

Fits of planet data to our model show that the base of the telescope is tilted about 20 arcseconds from the horizontal. Measurements with inclinometers confirm this number. Values for the other parameters show some degeneracy due to the fact that the planets, which are constrained to the ecliptic, cover a limited area of the celestial sphere.

Despite a lack of full convergence in the pointing model, it should be remarked that it is possible to correct pointing offsets by matching point sources in our maps to catalogue positions. This method will give complementary information for our pointing model, and may in fact make a high precision pointing model from planets unnecessary.

6. PRELIMINARY BEAM ANALYSIS

Fig. 6 is a coadded map of Saturn using a single six-minute observation and all working detectors. The solid angle in this map is about 215 nanosteradians (nsr) and the full width at half maximum (FWHM) is about 1.44 arcminutes.

Averaging beam maps from a few dozen Mars and Saturn observations, we find a solid angle of (216 ± 8) nsr and a FWHM of (1.44 ± 0.02) arcminutes. Our beam analysis is still being developed, and the uncertainties quoted in these parameters are dominated by systematic errors in the background subtraction. Nevertheless, the FWHM is known well enough to compare to a beam model. Integrating Airy functions from a 5.8 m aperture diameter over the 145 GHz bandpass, and then convolving with the shape of a square detector, predicts a FWHM of 1.38 arcminutes.[16] The choice of a 5.8 m aperture was motivated by the fact that our cold Lyot stop is designed to illuminate 97% of the six-meter primary mirror.[6]

The fact that the measured FWHM exceeds the modeled value can be attributed to two effects. First, the measured value is from a map that coadds detectors across the 145 GHz array, which should smear out the beam

slightly. Second, in reality, the primary and secondary mirrors are not uniformly illuminated. This effectively decreases the aperture size in the naive Airy model, and hence increases the FWHM of the beam, which goes as the inverse of the aperture size.

Our understanding of the beam is still preliminary at this time. More precise beam analysis coupled with more sophisticated modeling of the optics are still required. Fig. 6, together with qualitative comparison to the Airy model shows, however, that the telescope optics are performing well at a fundamental level.

7. CONCLUSIONS

After one season in the field, the ACT is now working. The azimuth scanning motion is sufficiently smooth at the speeds required for our observations. The mirror surfaces were successfully aligned, with the primary surface rms at 31 μm and the secondary at 10 μm. Seven months after alignment, both surfaces were measured to have an rms of 35 μm, demonstrating that the primary tolerance is retained well, while the change in the secondary needs to be investigated further. Thermal distortion of the structure did not permit observations between sunrise and sunset, but we have plans to minimize solar heating during the day for future observing seasons in an effort to extend the length of observations. Our pointing model confirms the measured base tilt of 20 arcseconds.

Reduction of the 2007 data is ongoing. Preliminary beam analysis shows that the optics are performing according to their design. We conclude that we have a functioning instrument which is capable of making an important contribution to CMB physics, and millimeter-wave astronomy at large.

ACKNOWLEDGMENTS

This results in this paper represent the work of a large group of people. We thank all of the employees of Dynamic Structures, KUKA Robotics, Forcier Machine Design, and Con Pax. Walter Brzezik (formerly DS), Cristián Pérez Rossi (Con Pax), Mel Yargeau (DS), and Ye Zhao (DS) provided essential oversight during the construction in Chile. David Woody gave an insightful review of our mirror panel and adjuster design. We thank Jeffrey Funke and Michael Gerstenberger of KUKA, and especially Michael Cozza, also of KUKA, who worked indefatigably at perfecting the telescope motion. We benefited greatly from the conversations, advice, and informal support from our colleagues at other experiments in the Atacama, namely, ALMA, APEX, ASTE, CBI, and Nanten.

This work was supported by the U.S. National Science Foundation through awards AST-0408698 for the ACT project and PHY-0355328. Funding was also provided by Princeton University and the University of Pennsylvania. A. Hincks received additional support from a Natural Science and Engineering Research Council of Canada (NSERC) PGS-D scholarship.

REFERENCES

1. Kosowsky, A., "The Atacama Cosmology Telescope," *New Astron. Rev.* **47**, 939–943 (2003).
2. Fowler, J. W., "The Atacama Cosmology Telescope Project," *Proc. SPIE* **5498**, 1–10 (2004).
3. Marriage, T. A., *Detectors for the Atacama Cosmology Telescope*, PhD thesis, Princeton University (2006).
4. Swetz, D. S., Ade, P. A. R., Allen, C., Amiri, M., Appel, J. W., Battistelli, E. S., Burger, B., Chervenak, J. A., Dahlen, A. J., Das, S., Denny, S., Devlin, M. J., Dicker, S. R., Doriese, W. B., Dünner, R., Essinger-Hileman, T., Fisher, R. P., Fowler, J. W., Gao, X., Hajian, A., Halpern, M., Hargrave, P. C., Hasselfield, M., Hilton, G. C., Hincks, A. D., Irwin, K. D., Jarosik, N., Kaul, M., Klein, J., Knotek, S., Lau, J. M., Limon, M., Lupton, R. H., Marriage, T. A., Martocci, K. L., Mauskopf, P., Moseley, S. H., Netterfield, C. B., Niemack, M. D., Nolta, M. R., Page, L., Parker, L. P., Reid, B. A., Reintsema, C. D., Sederberg, A., Sehgal, N., Sievers, J. L., Spergel, D. N., Staggs, S. T., Stryzak, O. R., Switzer, E. R., Thornton, R. J., Tucker, C., Wollack, E. J., and Zhao, Y., "Instrument design and characterization of the Millimeter Bolometer Array Camera on the Atacama Cosmology Telescope," *Also in these Proc. SPIE* .

5. Thornton, R. J., Ade, P. A. R., Allen, C., Amiri, M., Appel, J. W., Battistelli, E. S., Burger, B., Chervenak, J. A., Devlin, M. J., Dicker, S. R., Doriese, W. B., Essinger-Hileman, T., Fisher, R. P., Fowler, J. W., Halpern, M., Hargrave, P. C., Hasselfield, M., Hilton, G. C., Hincks, A. D., Irwin, K. D., Jarosik, N., Kaul, M., Klein, J., Lau, J. M., Limon, M., Marriage, T. A., Martocci, K., Mauskopf, P., Moseley, H., Niemack, M. D., Page, L., Parker, L. P., Reidel, J., Reintsema, C. D., Staggs, S. T., Stryzak, O. R., Swetz, D. S., Switzer, E. R., Tucker, C., Wollack, E. J., and Zhao, Y., "Optomechanical design and performance of a compact three-frequency camera for the MBAC receiver on the Atacama Cosmology Telescope," *Also in these Proc. SPIE* .
6. Fowler, J. W., Niemack, M. D., Dicker, S. R., Aboobaker, A. M., Ade, P. A. R., Battistelli, E. S., Devlin, M. J., Fisher, R. P., Halpern, M., Hargrave, P. C., Hincks, A. D., Kaul, M., Klein, J., Lau, J. M., Limon, M., Marriage, T. A., Mauskopf, P. D., Page, L., Staggs, S. T., Swetz, D. S., Switzer, E. R., Thornton, R. J., and Tucker, C. E., "Optical design of the Atacama Cosmology Telescope and the Millimeter Bolometric Array Camera," *Appl. Opt.* **46**(17), 3444–3454 (2007).
7. Zhao, Y., Allen, C., Amiri, M., Appel, J. W., Battistelli, E. S., Burger, B., Chervenak, J. A., Dahlen, A., Denny, S., Devlin, M. J., Dicker, S. R., Doriese, W. B., Dünner, R., Essinger-Hileman, T., Fisher, R. P., Fowler, J. W., Halpern, M., Hilton, G. C., Hincks, A. D., Irwin, K. D., Jarosik, N., Klein, J., Lau, J. M., Marriage, T. A., Martocci, K., Moseley, H., Niemack, M. D., Page, L., Parker, L. P., Sederberg, A., Staggs, S. T., Stryzak, O. R., Swetz, D. S., Switzer, E. R., Thornton, R. J., and Wollack, E. J., "Characterization of transition edge sensors for the Millimeter Bolometer Array Camera on the Atacama Cosmology Telescope," *Also in these Proc. SPIE* .
8. Niemack, M. D., Zhao, Y., Wollack, E., Thornton, R., Switzer, E. R., Swetz, D. S., Staggs, S. T., Page, L., Stryzak, O., Moseley, H., Marriage, T. A., Limon, M., Lau, J. M., Klein, J., Kaul, M., Jarosik, N., Irwin, K. D., Hincks, A. D., Hilton, G. C., Halpern, M., Fowler, J. W., Fisher, R. P., Dünner, R., Doriese, W. B., Dicker, S. R., Devlin, M. J., Chervenak, J., Burger, B., Battistelli, E. S., Appel, J., Amiri, M., Allen, C., and Aboobaker, A. M., "A kilopixel array of TES bolometers for ACT: Development, testing, and first light," *J. Low Temp. Phys.* **151**(3-4), 690–696 (2008).
9. Marriage, T. A., Chervenak, J. A., and Doriese, W. B., "Testing and assembly of the detectors for the Millimeter Bolometric Array Camera on ACT," *Nuc Inst & Meth. in Phys Res A* **559**, 551–553 (2006).
10. Battistelli, E. S., Amiri, M., Burger, B., Devlin, M. J., Dicker, S. R., Doriese, W. B., Dünner, R., Fisher, R. P., Fowler, J. W., Halpern, M., Hasselfield, M., Hilton, G. C., Hincks, A. D., Irwin, K. D., Kaul, M., Klein, J., Knotek, S., Lau, J. M., Limon, M., Marriage, T. A., Niemack, M. D., Page, L., Reintsema, C. D., Staggs, S. T., Swetz, D. S., Switzer, E. R., Thornton, R. J., and Zhao, Y., "Automated SQUID tuning procedure for kilopixel arrays of TES bolometers on ACT," *Also in these Proc. SPIE* .
11. Switzer, E. R., Allen, C., Amiri, M., Appel, J. W., Battistelli, E. S., Burger, B., Chervenak, J. A., Dahlen, A., Das, S., Devlin, M. J., Dicker, S. R., Doriese, W. B., Dünner, R., Essinger-Hileman, T., Fisher, R. P., Fowler, J. W., Gao, X., Halpern, M., Hasselfield, M., Hilton, G. C., Hincks, A. D., Irwin, K. D., Jarosik, N., Kaul, M., Knotek, S., Klein, J., Lau, J. M., Limon, M., Lupton, R., Marriage, T. A., Martocci, K., Moseley, H., Netterfield, B., Niemack, M. D., Nolta, M., Page, L., Parker, L. P., Reid, B., Reintsema, C. D., Sederberg, A., Sievers, J., Spergel, D., Staggs, S. T., Stryzak, O., Swetz, D. S., Thornton, R., Wollack, E., and Zhao, Y., "Systems and control software for the atacama cosmology telescope," *Also in these Proc. SPIE* .
12. Open DeviceNet Vendors Association (ODVA). Internet URL: http://www.odva.org/.
13. Rohlfs, K. and Wilson, T. L., [*Tools of Radio Astronomy*], Springer, 3rd ed. (2000).
14. Ruze, J., "Antenna tolerance theory – a review," *Proc. IEEE* **54**, 633–640 (1966).
15. Born, M. and Wolf, E., [*Principles of Optics*], Pergamon Press, 6th ed. (1980).
16. Niemack, M. D., *Towards Dark Energy: Design, Development, and Preliminary Data from ACT*, PhD thesis, Princeton University (2008).